

LASER FREQUENCY STABILIZATION TECHNIQUES & ITS APPLICATIONS

H. S. Boyne
Radio Standards Physics Division
National Bureau of Standards
Boulder, Colorado

(Contribution of National Bureau of Standards, not subject to copyright)

Abstract

A review of progress in laser stabilization techniques and laser frequency measurement is given. Methods for relating laser frequencies to the time standard and methods for absolute laser frequency stabilization are described. Experimental information on reproducibility and noise characteristics is reported. Application to frequency and wavelength standards is discussed.

Introduction

Since the discovery of the He-Ne gas laser in 1960 by Javan, Bennett and Herriot, many atomic and molecular laser transitions have been found. The possibility of using one of these transitions as a highly stable frequency or wavelength standard in the visible or near infrared has been envisioned, and many schemes have been developed to try to reproduce accurately the wavelength of one of these transitions.^{2,3,4} The usual techniques involve servo-control of the laser cavity to some characteristic of the laser transition. The major problems involved with these attempts were large frequency shift due to gas pressure changes in the plasma, amplitude and frequency fluctuations due to plasma instabilities, and the dependence of the frequency on the current-voltage characteristics of the plasma discharge.

In 1967 there were two important developments in laser spectroscopy that pointed the direction necessary to realize accuracy competitive with frequency standards--saturated absorption of atoms and molecules first reported by Lee and Skolnick⁵ and absolute frequency measurement of a laser transition first reported by Hocker et al.⁶

Saturated Absorption

The research of Lee and Skolnick on saturated absorption in Ne led others, namely

Barger and Hall,⁷ Hanes and Baird,⁸ and Rabinowitz et al,⁹ into the investigation of saturated absorption of molecular species having absorption transitions coincident with the laser transition. The molecular species that have been reported to date are I₂, CH₄, and SF₆. Molecular species are attractive because molecular vibration-rotation transitions have characteristically long lifetimes, absorption can be obtained from thermally populated states, and there is a much higher probability for coincidences of a molecular transition with a laser transition. The most extensive research to date has been done on I₂ and CH₄.

The principle of saturated absorption can be illustrated by referring to Fig. 1. A cell containing the absorbing gas is placed inside the laser cavity. The absorption transition whose Doppler width is greater than the natural line width interacts with the laser radiation such that absorption takes place at the laser frequency $f = f_0(1 \pm v_z/c)$ where f_0 is the molecular transition frequency at rest and v_z is the speed of the molecule along the laser axis. If we think of the standing wave laser radiation pattern as composed of two oppositely directed running waves of equal amplitude, then two holes are "burned out" of the absorption density distribution as a function of velocity. The width of these holes is proportional to the natural width of the absorbing transition so that when the absorption is away from the central peak the two populations act almost independently. As the laser frequency is tuned to the absorption line center, however, the same molecules interact with both running waves and saturation occurs. This leads to an increased power output at frequency f_0 . The emission peak at f_0 has a characteristic width γ where $1/\gamma$ may be the collision induced lifetime, the natural lifetime, or the transit time of the molecule across the laser beam, whichever is the shortest characteristic time. The output intensity is $I = I_0[1 + \mathcal{L}(f - f_0, \gamma)]$ where \mathcal{L} is a Lorentzian function and $f - f_0$ is the frequency measured from line center. Fig. 2 shows the

power versus frequency curve for saturated absorption of methane at 3.39μ . The absorption is that of a single transition which is the P7 line of the ν_3 vibration band in methane. The laser transition has been pressure shifted to higher frequency by approximately 100 MHz to make the centers of the P7 transition and the 3.39μ Ne transition coincide. The line width is approximately 200 KHz. The broadening of this line has been studied extensively in both pure CH_4 and in CH_4 with the rare gases as buffers. The width of the absorption in pure methane as a function of pressure is approximately 10 KHz per micron. By using special "frequency offset locking" described by Barger and Hall,⁷ pressure shift of the methane transition can be investigated. This shift is anomalously small for reasons which are not clearly understood at this time. The shift as a function of pressure is given by Barger and Hall⁷ as 75 ± 150 Hz per micron. Two independent methane stabilized lasers have been investigated and a stability plot of the difference frequency between the two lasers as a function of time is shown in Fig. 3. Recent improvements on this stability have been made and will be reported elsewhere.¹⁰ More recent stability measurements show that the methane stabilized laser may be competitive with the hydrogen maser.

Other experiments dealing with the saturated absorption of I_2 at 633 nm and the saturated absorption of SF_6 at 10.6μ have been reported.^{8,11} The power tuning curve for saturated absorption of I_2 is shown in Fig. 4. The lower trace in the figure is the derivative of the power curve which has an approximate Lorentzian shape. The several absorptions seen are due to the hyperfine structure in I_2 . Fig. 5 shows the absorption of SF_6 from the P18 line of the CO_2 laser.⁹ Because of the very high power output, the absorption can be seen with a cell outside the laser cavity in which the radiation is double-passed to achieve a standing wave pattern.

Frequency Synthesis

Table 1 shows the frequencies involved in attempting to establish a frequency locked chain from a stabilized klystron to the near infrared. The initial measurements in this chain were accomplished by Hocker et al⁶ who mixed the 12th harmonic of a 74 GHz klystron with the 337μ HCN laser. The next step in the chain has been accomplished by Evenson et al¹² in mixing the 12th harmonic of 337μ with the 27μ water vapor laser. The most recent accomplishment

has been to mix the 3rd harmonic of 27μ with the 9.3μ transition in CO_2 by Daneu et al¹³ and the mixing of the 3rd harmonic of 27μ minus the 1st harmonic of 78μ to measure both the P18 and P20 transitions of CO_2 laser by Evenson et al.¹⁴ All of these measurements have been accomplished by using a cat whisker diode detector. Fig. 6 shows an exploded view of the cat whisker which is usually made out of tungsten and is pointed by chemical etching techniques. The post which makes contact with the whisker can be either silicon as was the case for the first experiments by Hocker et al,⁶ or can be some form of metal post as is the case for the more recent experiments.^{13,14} The whisker acts as a long wave antenna as has been shown by Matarrese and Evenson.¹⁵ Number of lobes of the antenna pattern is proportional to the length of the whisker divided by the wavelength of the radiation. Fig. 7 displays this pattern for $L = 7\lambda$.

Attempts are currently being made to mix the 8th harmonic of the 27μ H_2O vapor laser with the 3.39μ He-Ne laser. If this step can be accomplished, a frequency locked chain from the time standard to 3.39μ can be established and the stability of the saturated absorption at 3.39μ strongly suggests that this transition could be used as a new primary length standard. This being the case, the length standard and the time standard could be compared directly. If the primary length and time standard could be derived from the same atomic or molecular transition, the speed-of-light would become a defined quantity and length measurement could be derived from frequency measurements.

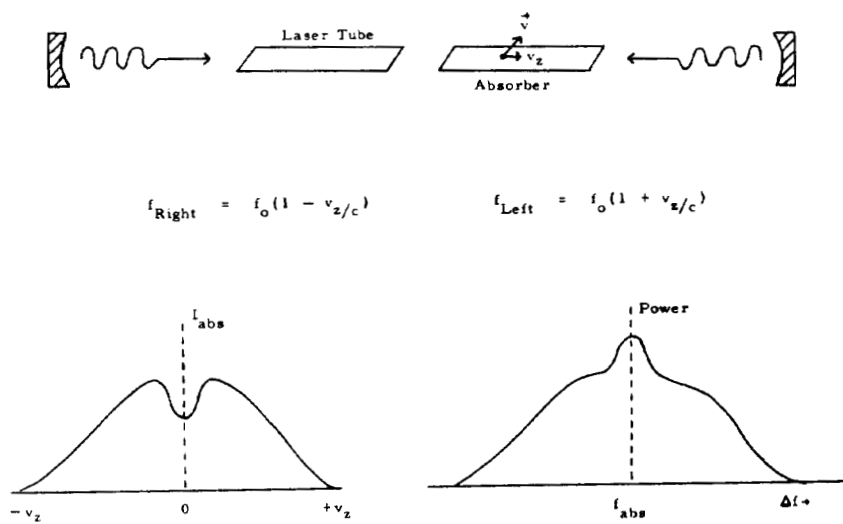
Acknowledgement

It is a pleasure to acknowledge cooperation given to me prior to publication by Drs. Barger, Hall, and Evenson in supplying data and helpful suggestions for this report. It is also a pleasure to acknowledge cooperation by Dr. Rabinowitz and Dr. Hanes in allowing photographs of their research to be published.

References

1. A. Javan, W. R. Bennett, Jr., and D. R. Herriot, *Physical Review Letters* **6**, p. 3 (1961).
2. A. D. White, *IEEE Journal of Quantum Electronic*, QE-1, p. 349 (1965).

3. G. Birnbaum, Proceedings of the **IEEE** 55, p. 1015 (1967).
4. J. L. Hall, **IEEE Journal of Quantum Electronics**, QE-4, p. 638 (1968).
5. P. L. Lee and M. L. Skolnick, **Applied Physics Letters** 10, p. 303 (1967).
6. L. O. Hocker, A. Javan, D. Ramachandra Rao, L. Frenkel and T. Sullivan, **Applied Physics Letters** 10, p. 147 (1967).
7. R. L. Barger and J. L. Hall, **Physical Review Letters** 22, p. 4 (1969).
8. G. R. Hanes and K. M. Baird, **Metrologia** 5, p. 32 (1969).
9. P. Rabinowitz, R. Keller, and J. T. LaTourrette, **Applied Physics Letters** 14, p. 376 (1969).
10. J. L. Hall and R. L. Barger, to be published. (Also see: R. L. Barger and J. L. Hall, Proceedings of the 23rd Annual Symposium on Frequency Control, p. 306, 1969.)
11. G. R. Hanes and C. E. Dahlstrom, **Applied Physics Letters** 14, p. 362 (1969).
12. K. M. Evenson, J. S. Wells, L. M. Matarrese, and L. B. Elwell, **Applied Physics Letters** 16, p. 159 (1970).
13. V. Daneu, D. Sokoloff, A. Sanchez, and A. Javan, **Applied Physics Letters** 15, p. 398 (1969).
14. K. M. Evenson, J. S. Wells, and L. M. Matarrese, **Applied Physics Letters** 16, p. 251 (1970).
15. L. M. Matarrese and K. M. Evenson, **Applied Physics Letters**, to be published.



SATURATED ABSORPTION

Fig. 1 - Saturated absorption explained as the interaction of two running waves with the absorbing medium.

© 1964

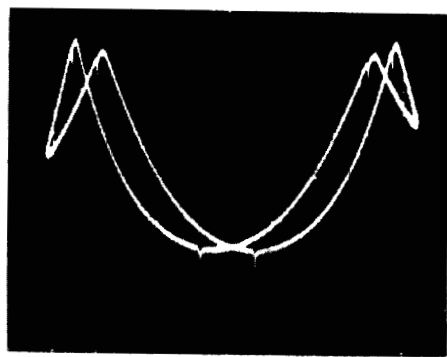


Fig. 2 - Saturated absorption in methane at 3.39μ .

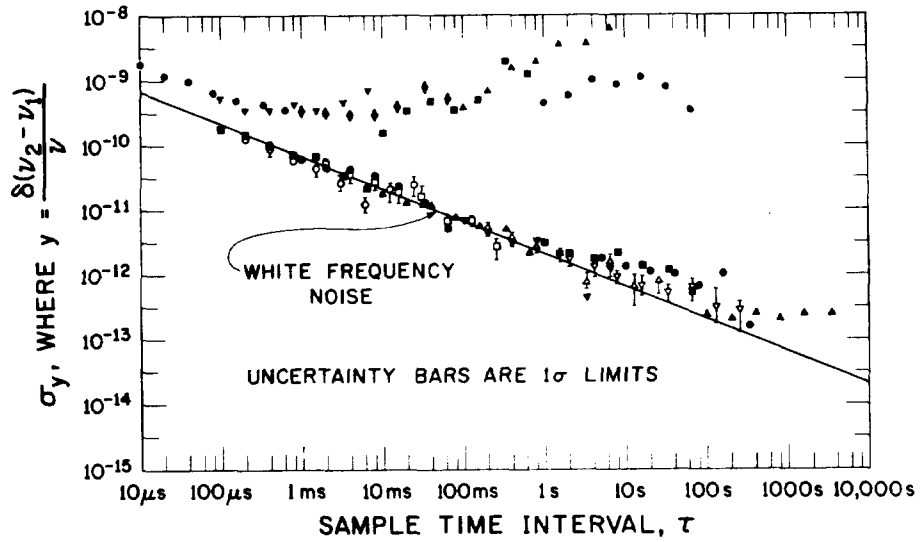


Fig. 3 - Plot of beat frequency stability between two independently stabilized methane lasers as a function of sample time.

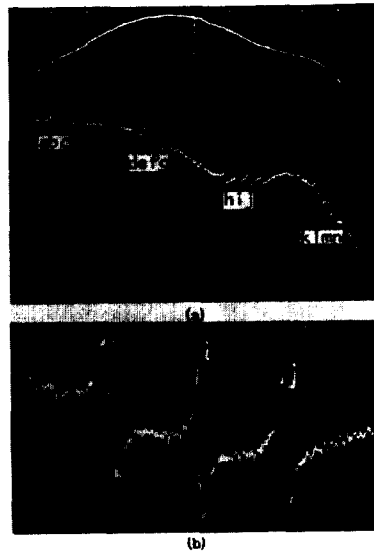


Fig. 4 - (a) Composite photograph showing laser power output versus tuning in the upper trace, and the derivative of power with respect to cavity length in the lower trace. Dispersion is approximately 50 MHz per division. Red is on the right. The labelled discriminant curves are due to the presence of iodine vapour in the laser cavity. (b) Enlarged view of three of the components at 5 MHz/division.

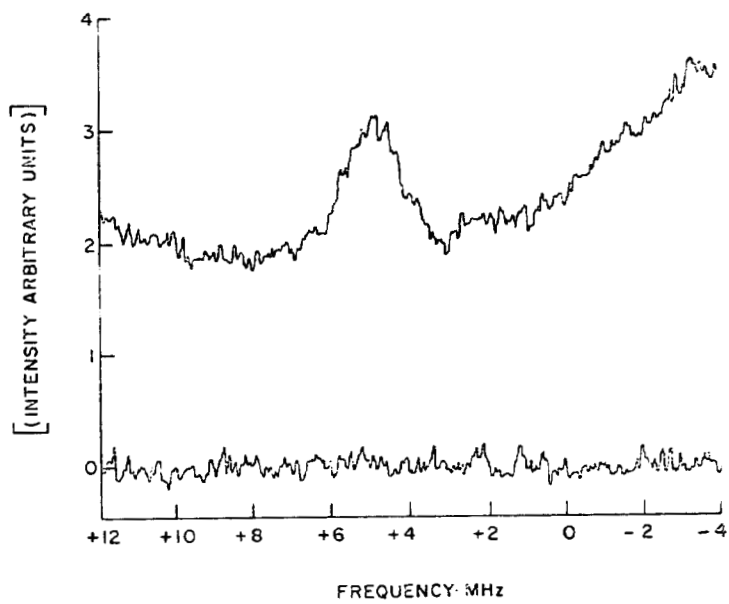


Fig. 5 - Saturated absorption of SF_6 for the P18 transition of the CO_2 laser.



Fig. 6 - View of whisker diode. Metal post is to the left of the whisker. Large vertical post is the mount for the figure.

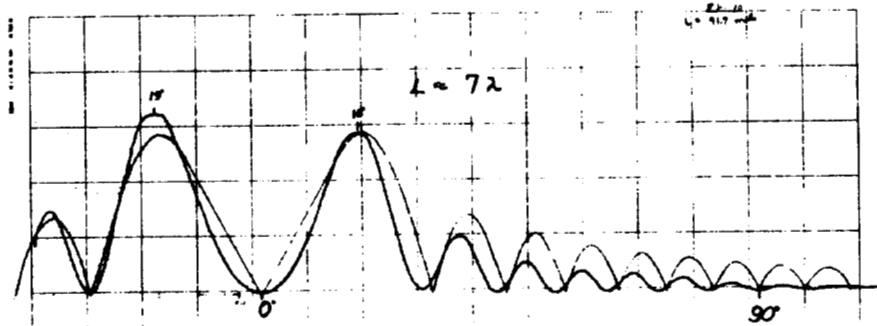


Fig. 7 - Antenna radiation pattern for length of wire 7λ . Solid line is experimental curve. -- line is theoretically predicted curve.

$$\nu_x = n\nu_1 + m\nu_2 + l\nu_3 + \nu_{\text{beat}} \text{ (30 MHz)}$$

ν_x	λ_x	Laser		Laser		Klystron	
		n	ν_1	m	ν_2	l	ν_3
.8907606 ^A	337μ					12	.0742
3.821775 ^B	78μ	6	.891	-2	.805	3	.029
10.718073 ^B	28μ	12	.891			1	.029
28.359800 ^B	10.6μ	3	10.710	-1	3.821	1	.027
28.306251 ^B	10.6μ	3	10.710	-1	3.821	-1	.026
32.176084 ^A	9.3μ	3	10.710			1	.022
32.134269 ^A	9.3μ	3	10.710			-1	.020
88.37637 ^B	3.39μ	8	10.710	3	.891	-1	.040

Table 1 - Frequency multiplication steps necessary to achieve frequency synthesis to the near infrared. A--represents measurements done at MIT. B--represents measurements done at NBS, Boulder. B--proposed measurement.